Journal of Alloys and Compounds 509 (2011) L183–L186

Contents lists available at ScienceDirect

Journal of Alloys and Compounds

journal homepage: www.elsevier.com/locate/jallcom

Letter

Fast consolidation of a nanocrystalline Al_2O_3 reinforced $3.7Fe_{0.54}Cr_{0.18}Al_{0.26}Si_{0.016}$ composite from mechanical synthesized powder through pulsed current activated heating

In-Jin Shon[a,*], Seung-Hoon Jo[a], In-Yong Ko[a], Jung-Mann Doh[b], Jin-Kook Yoon[b], Sang-Whan Park[b]

[a] Division of Advanced Materials Engineering and Research Center of Advanced Materials Development, Engineering College, Chonbuk National University, Chonbuk, 561-756, Republic of Korea

[b] Advanced Functional Materials Research Center, Korea Institute of Science and Technology, PO Box 131, Cheongryang, Seoul 130-650, Republic of Korea

ARTICLE INFO

Article history:
Received 24 December 2010
Received in revised form 23 February 2011
Accepted 28 February 2011

Keywords:
Nanostructured materials
Sintering
Mechanical alloying
Hardness
Composite materials

ABSTRACT

Nanopowders of $Fe_{0.54}Cr_{0.18}Al_{0.26}Si_{0.016}$ and Al_2O_3 were synthesized from Fe_2O_3, Cr, Si, and Al powders using high-energy ball milling. A high-density nanocrystalline $3.7Fe_{0.54}Cr_{0.18}Al_{0.26}Si_{0.016}$–$Al_2O_3$ composite was consolidated with mechanically synthesized powders of Al_2O_3 and $3.7Fe_{0.54}Cr_{0.18}Al_{0.26}Si_{0.016}$–$Al_2O_3$ through a pulsed current activated sintering (PCAS) method within 1 min. The hardness of the composite and the average grain sizes of Al_2O_3 and $Fe_{0.54}Cr_{0.18}Al_{0.26}Si_{0.016}$ were investigated.

1. Introduction

It is increasingly being recognized that new material applications require functions and properties that are not achievable with monolithic materials. Metal matrix composites combine metallic properties (ductility and toughness) with ceramic characteristics (high strength and modulus), leading to greater strength in shear and compression and higher service temperature capabilities. The attractive physical and mechanical properties that can be obtained with metal matrix composites, such as high specific modulus, strength-to-weight ratio, fatigue strength, temperature stability and wear resistance, have been documented extensively [1–5]. As a result, metal matrix composites are recognized as candidates for aerospace, automotive, biomaterial and defense applications.

Iron–aluminium–chromium–silicon alloys are applicable as structural materials and as coatings for high-temperature applications [6]. Their excellent corrosion resistance is due to the formation of a dense, protective alumina scale coating. Alumina (α-Al_2O_3 in particular) demonstrates a low rate constant, even at temperatures above 1000 °C [7].

However, like many alloys, the applications of iron–aluminium–chromium–silicon alloys in industry have been limited due to low hardness. The hardness can be improved significantly through reinforcement with hard ceramic particles, such as Al_2O_3 [8], and through the fabrication of nanostructured composites [9]. Al_2O_3 has a density of 3.98 g/cm^3, Young's modulus of 380 GPa, excellent oxidation resistance and good high-temperature mechanical properties [10]. Hence, a microstructure consisting of a FeAlCrSi alloy and Al_2O_3 may satisfy the oxidation resistance and high temperature mechanical property requirements of a high-temperature structural material.

Discontinuously reinforced metal matrix composites have been produced using several processes, including powder metallurgy, spray deposition, mechanical alloying, casting, and self-propagating high-temperature synthesis (SHS). A technique that uses high-energy ball milling and mechanical alloying of powder mixtures (which is a combination of mechanical milling and chemical reactions) has been reported as an efficient method for preparing nanocrystalline metals and alloys [11].

Nanocrystalline materials have received much attention in the advancement of engineering materials due to their improved physical and mechanical properties [12,13]. Nanomaterials typically possess high strength, high hardness, excellent ductility, and toughness. Therefore, increasing attention has been paid to the development of potential nanomaterial applications [14]. The grain sizes in sintered materials are much larger than those in pre-sintered powders due to the fast grain growth that occurs during conventional sintering processes. Therefore, even though

* Corresponding author. Tel.: +82 63 2381; fax: +82 63 270 2386.
E-mail address: ijshon@chonbuk.ac.kr (I.-J. Shon).

0925-8388/$ – see front matter © 2011 Elsevier B.V. All rights reserved.
doi:10.1016/j.jallcom.2011.02.172

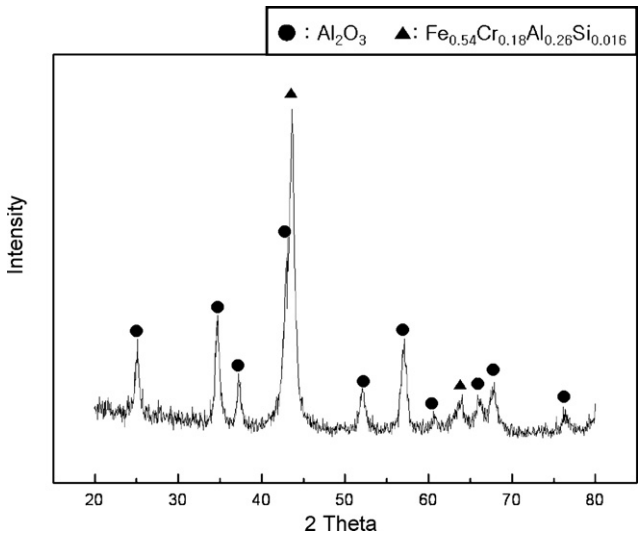

Fig. 1. XRD pattern of the mechanically alloyed $3.7Fe_{0.54}Cr_{0.18}Al_{0.26}Si_{0.016}$–$Al_2O_3$ powder.

the initial particle size is less than 100 nm, the grain size rapidly increases up to 2 μm or larger during conventional sintering [15]. As a result, controlling the grain growth during sintering is a key to the commercial success of nanostructured materials. Pulsed current activated sintering methods, which can be used to rapidly manufacture dense materials within 2 min, can effectively control the grain growth [16,17].

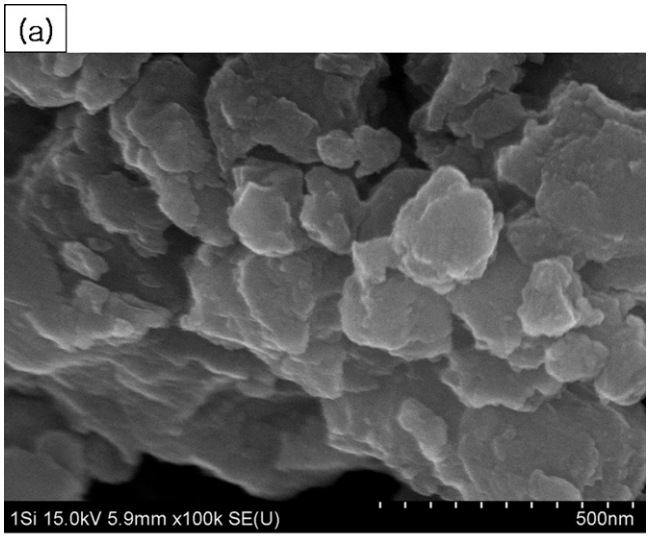

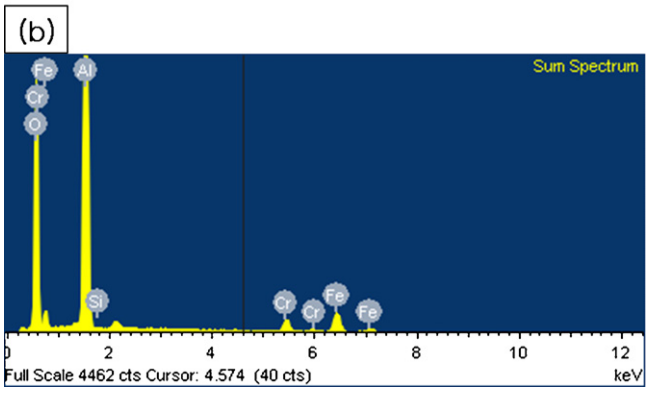

Fig. 2. FE-SEM image of the $3.7Fe_{0.54}Cr_{0.18}Al_{0.26}Si_{0.016}$–$Al_2O_3$ composite, and X-ray mapping of O, Al, Si, Fe, and Cr.

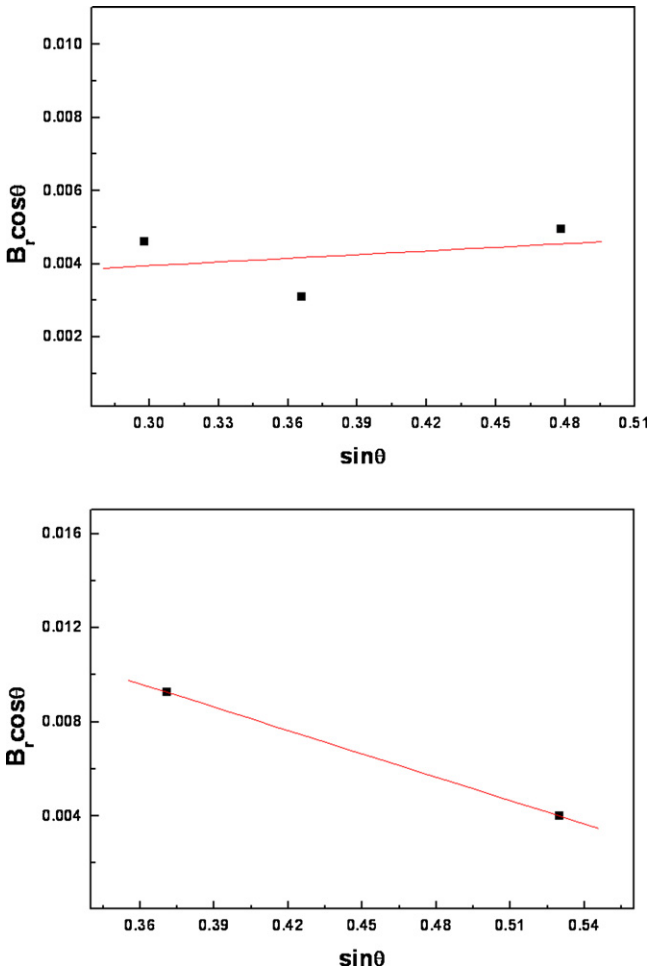

Fig. 3. Plots of $B_r\cos\theta$ versus $\cos\theta$ for $3.7Fe_{0.54}Cr_{0.18}Al_{0.26}Si_{0.016}$ and Al_2O_3 in the mechanically alloyed powders.

The goals of this work were to fabricate a new nanopowder using high-energy ball milling, produce a dense nanocrystalline Al_2O_3-reinforced Fe–Cr–Al–Si composite from mechanically alloyed powders within 1 min via pulsed current activated sintering method and to evaluate its hardness and grain size.

2. Experimental procedures

Powders of 99% pure Fe_2O_3 (<5 μm, Alfa Co.), 99.5% pure Al (<325 mesh, Alfa Co.), 99.5% pure Si (<325 mesh, Alfa Co.), and 99.8% pure Cr (<10 μm, Alfa Co.) were used as the starting materials. Fe_2O_3, 0.67Cr, 0.06Si, and 2.96Al powder mixtures were milled in a high-energy ball mill (Pulverisette 5 planetary mill) at 250 rpm for 10 h to produce $Al_2O_3 + 3.7Fe_{0.54}Cr_{0.18}Al_{0.26}Si_{0.016}$. Tungsten carbide balls (8.5 mm in diameter) were used in a sealed cylindrical stainless steel vial under an argon atmosphere. The weight ratio of balls to powder was 30:1. Milling resulted in a significant reduction of grain size, the magnitudes of which were calculated using Suryanarayana's and Norton's formula [18]:

$$B_r(B_{crystalline} + B_{strain})cos\theta = \frac{k\lambda}{L + \eta\sin\theta}, \quad (1)$$

where B_r is the full width at half-maximum (FWHM) of the diffraction peak after instrument correction, $B_{crystalline}$ and B_{strain} are the FWHM values caused by the small grain size and internal stress, respectively, k is a constant of 0.9, λ is the wavelength of the X-ray radiation, L is the grain size, η is the internal strain, and θ is the Bragg angle. The parameters B and B_r follow Cauchy's form with the relationship $B = B_r + B_s$, where B and B_s are the FWHM values of the broadened Bragg peaks and the standard sample's Bragg peaks, respectively.

After milling, the mixed powders were placed in a graphite die (external diameter of 45 mm, inner diameter of 20 mm, height of 40 mm) and then introduced into

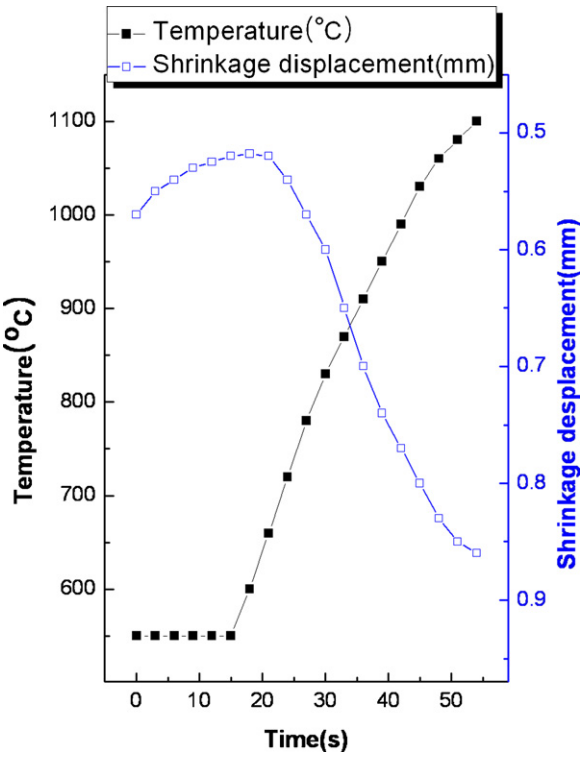

Fig. 4. Variations in temperature and shrinkage displacement with heating time during pulsed current activated sintering of $3.7Fe_{0.54}Cr_{0.18}Al_{0.26}Si_{0.016}$–$Al_2O_3$ powders.

a pulsed current (on time; 20 μs, off time; 10 μs) activated sintering system (Eltek, South Korea), shown schematically in [16,17]. The four major stages in the synthesis were evacuation of the system, application of uniaxial pressure, heating of the sample by an induced current, and cooling of the sample. The process was conducted under a vacuum of 40 mTorr.

Microstructural information was obtained from product samples that were polished at room temperature. Compositional and microstructural analyses of the products were conducted using X-ray diffraction (XRD) and a scanning electron microscope (SEM) with energy dispersive X-ray analysis (EDAX). The Vickers hardness was measured by performing indentations on the sintered samples at a load of 10 kg and a dwell time of 15 s.

3. Results and discussion

Fig. 1 shows the XRD results for the high-energy, ball-milled powders. Fe_2O_3, Cr, Si, and Al reactant powders were not detected, while the Fe–Cr–Al–Si alloy and Al_2O_3 were detected. Based on the above results, the mechanical alloy was completely formed during milling. The net reaction can be considered a combination of the following two reactions:

$$Fe_2O_3 + 2Al \rightarrow 2Fe + Al_2O_3 \quad (2)$$

$$2Fe + 0.67Cr + 2.96Al + 0.06Si \rightarrow 3.7Fe_{0.54}Cr_{0.18}Al_{0.26}Si_{0.016} \quad (3)$$

Reaction (2) is the exothermic reaction for which the standard enthalpy of reaction ranges from −847 kJ to −811 kJ over the temperature range of 700 °C (just above the melting temperature of Al, 660 °C) to 1500 °C (just below the melting point of Fe, 1536 °C).

Fig. 2 shows an FE-SEM image and EDS results of high-energy, ball-milled powders. The powders were very fine agglomerations. Atoms of Fe, Cr, Al, Si and O were detected with EDS. The particle size could not be calculated using the linear intercept method due to the agglomeration of powders. Fig. 3 shows a plot of $B_r \sin\theta$ as a function of $\cos\theta$ to calculate the particle size using Suryanarayana's and Norton's formula [18]. The intercept ($K\lambda/L$) was used to calculate the crystallite size (L). The average grain sizes of Fe–Cr–Al–Si and

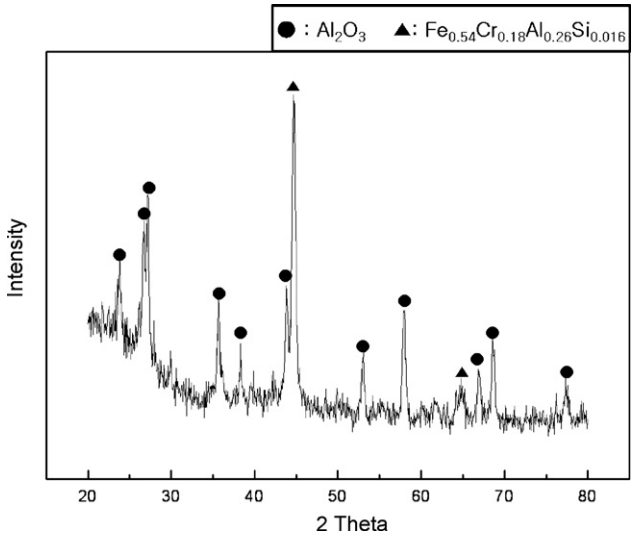

Fig. 5. XRD patterns of the $3.7Fe_{0.54}Cr_{0.18}Al_{0.26}Si_{0.016}$–$Al_2O_3$ composite heated to 1100 °C.

Al_2O_3, as determined using Suryanarayana's and Norton's formula, were approximately 6 nm and 47 nm, respectively.

Fig. 4 shows the variations in the shrinkage displacement and surface temperature of the graphite die with heating time during the processing of the Fe–Cr–Al–Si and Al_2O_3 system. When a pulsed current was applied, the specimen experienced thermal expansion, and the shrinkage displacement slowly increased to approximately 800 °C, then increased abruptly at approximately 1100 °C. As shown in Fig. 5, the XRD pattern of a sample heated to 1100 °C showed evidence of Fe–Cr–Al–Si alloy and Al_2O_3. An FE-SEM image of the $3.7Fe_{0.54}Cr_{0.18}Al_{0.26}Si_{0.016}$–$Al_2O_3$ composite is shown in Fig. 6, indicating that the structure consisted of nanophases with no pores. Thus, a nearly fully dense nanocomposite was obtained. Fig. 7 shows a plot of $B_r \cdot \cos\theta$ versus $\sin\theta$ used to calculate the structure parameters, including the average grain sizes of the Fe–Cr–Al–Si alloy and Al_2O_3. The grain sizes of the Fe–Cr–Al–Si alloy and Al_2O_3 obtained from the XRD data and Suryanarayana's and Norton's formula were 22 nm and 48 nm, respectively. The average grain sizes of the sintered Fe–Cr–Al–Si alloy and Al_2O_3 were not significantly larger than those of the initial powders, indicating the absence of significant grain growth during sintering. The retention of the grain size was attributed to the fast heating rate and relatively short

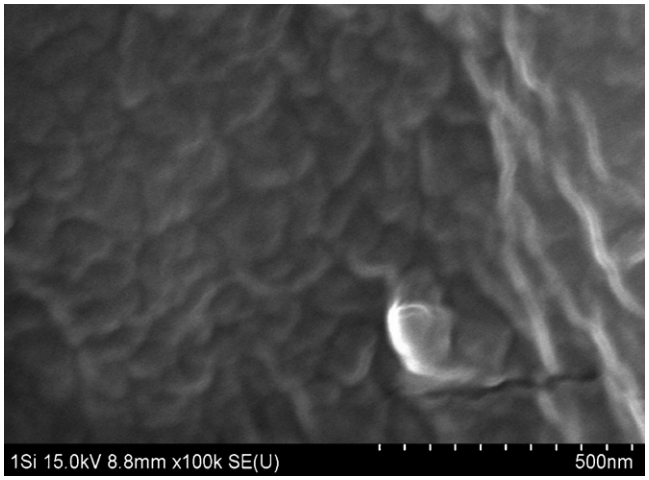

Fig. 6. FE-SEM image of the $3.7Fe_{0.54}Cr_{0.18}Al_{0.26}Si_{0.016}$–$Al_2O_3$ composite heated to 1100 °C.

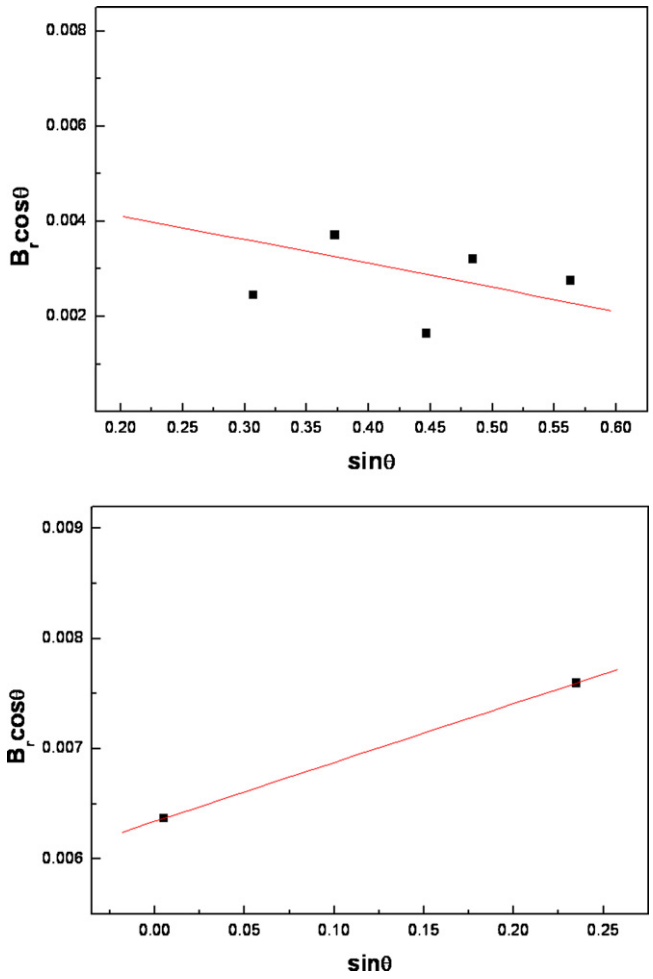

Fig. 7. Plots of $B_r \cos\theta$ versus $\cos\theta$ for $5.33Fe_{0.37}Cr_{0.16}Al_{0.4}Si_{0.07}$ and Al_2O_3 in the composite sintered at 1100 °C.

exposure of the powders to the high temperature. The role of current in sintering has been the focus of several attempts to explain the enhanced sintering and improved characteristics of the products. The current effect has been interpreted in terms of the fast heating rate due to Joule heating, the presence of plasma in pores separating powder particles, and the intrinsic contribution of the current to mass transport [19–22].

Vickers hardness measurements were performed on polished sections of the $3.7Fe_{0.54}Cr_{0.18}Al_{0.26}Si_{0.016}$–$Al_2O_3$ composite using a 10 kg_f load and a 15 s dwell time. The calculated hardness value of the $3.7Fe_{0.54}Cr_{0.18}Al_{0.26}Si_{0.016}$–$Al_2O_3$ composite was 450 kg/mm^2, an average of five measurements. The hardness was equated to the fracture toughness of the $3.7Fe_{0.54}Cr_{0.18}Al_{0.26}Si_{0.016}$–$Al_2O_3$ composite because no cracks were formed near the indent. The absence of reported hardness and toughness values for the $3.7Fe_{0.54}Cr_{0.18}Al_{0.26}Si_{0.016}$–$Al_2O_3$ composite precludes direct comparisons to the results obtained in this study. However, the hardness and fracture toughness of Al_2O_3 with a grain size of 4.5 μm were previously reported as 1800 kg/mm^2 and 4 MPa $m^{1/2}$, respectively [23]. The hardness of the $3.7Fe_{0.54}Cr_{0.18}Al_{0.26}Si_{0.016}$–$Al_2O_3$ composite was less than that of monolithic Al_2O_3, but the fracture toughness was greater due to the addition of the ductile Fe–Cr–Al–Si alloy.

4. Conclusions

Nanopowders of $Fe_{0.54}Cr_{0.18}Al_{0.26}Si_{0.016}$ and Al_2O_3 were fabricated from Fe_2O_3, Cr, Si, and Al powders using high-energy ball milling. The average grain sizes of the $3.7Fe_{0.54}Cr_{0.18}Al_{0.26}Si_{0.016}$ alloy and Al_2O_3 prepared via PCASM were 7 nm and 47 nm, respectively. Densification of a nanostructured $3.7Fe_{0.54}Cr_{0.18}Al_{0.26}Si_{0.016}$–$Al_2O_3$ composite prepared from mechanically alloyed powders was accomplished using the PCASM. Complete densification was achieved within a processing time of 3 min under an applied pressure of 80 MPa and an induced current. The average grain sizes of the $Fe_{0.54}Cr_{0.18}Al_{0.26}Si_{0.016}$ alloy and Al_2O_3 prepared through PCASM were approximately 22 nm and 48 nm, respectively, and the average hardness value was 450 kg/mm^2.

Acknowledgement

This work was supported by the New & Renewable Energy R&D Program (2009T00100316) of the Ministry of Knowledge Economy, Republic of Korea.

References

[1] J.S. Moya, S. Lopez-Esteban, C. Pecharroman, Prog. Mater. Sci. 52 (2007) 1017–1090.
[2] L. Ceschini, G. Minak, A. Morri, Compos. Sci. Technol. 66 (2006) 333–339.
[3] S.C. Tjong, Z.Y. Ma, Mater. Sci. Eng. 29 (2000) 49–55.
[4] D.J. Lloyd, Int. Mater. Rev. 39 (1) (1994) 1–6.
[5] J.M. Torralba, F. Velasco, J. Mater. Process. Technol. 133 (1–2) (2003) 03–206.
[6] J. Klower, Mater. Corros. 47 (1996) 685–694.
[7] P. Kofstad, High Temperature Corrosion, Elsevier Appl. Sci. Publ., London, New York, 1988.
[8] A. Michalski, J. Jaroszewicz, M. Rosinski, D. Siemiaszko, Intermetallics 14 (2006) 603–606.
[9] L.Z. Zhou, J.t. Guo, G.s. Li, L.Y. Xiong, S.H. Wang, C.G. Li, Mater. Des. 18 (1997) 373–377.
[10] M.F. Ashby, D.R.H. Jones, Engineering Materials 1 (International Series on Materials Science and Technology, Vol.34), Pergamon Press, Oxford, 1986.
[11] S. Paris, E. Gaffet, F. Bernard, Z.A. Munir, Scripta Mater. 50 (2004) 691–696.
[12] M.S. El-Eskandarany, J. Alloys Compd. 305 (2000) 225–238.
[13] L. Fu, L.H. Cao, Y.S. Fan, Scripta Mater. 44 (2001) 1061–1068.
[14] S. Berger, R. Porat, R. Rosen, Prog. Mater. Sci. 42 (1997) 311–320.
[15] J. Jung, S. Kang, Scripta Mater. 56 (2007) 561–564.
[16] H.C. Kim, I.J. Shon, I.J. Jeong, I.Y. Ko, J.K. Yoon, J.M. Doh, Met. Mater. Int. 13 (2007) 39–46.
[17] H.C. Kim, I.J. Shon, I.K. Jeong, I.Y. Ko, Met. Mater. Int. 12 (2006) 393–399.
[18] C. Suryanarayana, M. Grant Norton, X-Ray Diffraction: A Practical Approach, Plenum Press, 1998, p. 213.
[19] Z. Shen, M. Johnsson, Z. Zhao, M. Nygren, J. Am. Ceram. Soc. 85 (2002) 1921–1927.
[20] J.E. Garay, U. Anselmi-Tamburini, Z.A. Munir, S.C. Glade, P. Asoka- Kumar, Appl. Phys. Lett. 85 (2004) 573–575.
[21] J.R. Friedman, J.E. Garay, U. Anselmi-Tamburini, Z.A. Munir, Intermetallics 12 (2004) 589–597.
[22] J.E. Garay, U. Anselmi-Tamburini, Z.A. Munir, Acta Mater. 51 (2003) 4487–4495.
[23] Mohamed N. Rahaman, Aihua. Yao, B. Sonny Bal, Jonathan P. Garino, Michael D. Ries, J. Am. Ceram. Soc. 90 (2007) 1965–1988.